 DOI:10.30420/566414074

Power cycling lifetime model of sliver sintered SiC MOSFET power module based on physics-of-failure approach

Jie Chen[1,2], Wangjun Zhou[1,2], Zhexiong Luo[1,2], Haihui Luo[1,2], Qiang Xiao[1,2], Yadong Ren[1,2]

[1] Zhuzhou CRRC Times Semiconductor Co., Ltd., Hunan, China

[2] State Key Laboratory of Power Semiconductor and Integration Technology, Hunan, China

Corresponding author: Jie Chen, chenjie6@csrzic.com

Abstract

With the application of new packaging materials such as sintered silver in SiC modules, the high reliability characteristics poses new challenges to the product reliability evaluation, especially the lifetime modeling. Traditional modeling methods have problems such as time consumption and poor reusability, and the physics-of-failure methodology is used in this paper to infer fast lifetime prediction in early design stages. Firstly, a liquid-to-liquid thermal shock test was used to conduct an accelerated fatigue test, and the degradation of the sintered layer is quantitatively characterized through SAM images, then the fatigue model parameters are inverted combining finite element (FE) simulation and experiments. Finally, the electrical-thermal-mechanical FE model of the power module is established to simulate different power cycling conditions, and a lifetime model is established based on the predicted lifetime. The research methods and results can provide guidance for lifetime modeling and reliability forward design of power modules.

1 Introduction

In theory, the operating temperature of SiC devices can reach up to 500 ℃, but due to the constraints of packaging materials, they cannot perform their high-temperature characteristics [1]. For example, the melting point of commonly used SnAgCu solder is only 220 ℃, and the highest operating junction temperature of devices using solder is difficult to exceed 200 ℃. Therefore, it can be considered that packaging materials are the main reason limiting SiC devices in high-temperature applications. Additionally, the Young's modulus of SiC is about three times that of Si, resulting in a shorter thermal fatigue lifetime of SiC devices. Under the same packaging system, the power cycling lifetime of SiC devices is about 1/3 of that of Si devices [2].To meet the high temperature and high reliability requirements of SiC devices, nano sintered silver has become a new packaging material instead of solder.

Due to the higher electrical conductivity, thermal conductivity, and melting point of sintered silver, it has better electric-thermal properties and a longer lifetime compared to solder under the same thermal stress. In [3], the power cycling lifetime of the sintered layer under ΔT_j=120K can reach 440000 cycles, which is nearly 10 times longer than that of traditional Si devices. Such a high power cycling lifetime poses a huge challenge for lifetime modeling. On the one hand, it will significantly increase testing time, excessively consume testing resources, and on the other hand, it will prolong the product development cycle and reduce development efficiency. Therefore, new ideas and methods need to be introduced for power cycling lifetime modeling of sintered layers. In [4], a multidisciplinary cross disciplinary relationship diagram for reliability research of power electronic devices is provided , pointing out that physics of failure (POF) is the foundation of reliability research. The concept of POF was first formally proposed by the Rom Aviation Development Center of the United States Air Force in 1962. It refers to a method of predicting product reliability through simulation and modeling based on failure mechanism analysis [5]. Therefore, the modeling method based on POF is adopted in this paper to establish the power cycling lifetime model of SiC MOSFET power module.

2 Theory and model formulation

2.1 Viscoplastic constitutive model

Due to the mismatch of coefficients of thermal expansion (CTE) between different packaging materials, thermal stress is generated during temperature changes, leading to deformation. The total strain can be divided into three parts: elastic strain, plastic strain, and creep strain, which exist in different components during the fatigue process of the power module. For metal materials, such as aluminum bond wires, the strain is mainly composed of elastic strain and plastic strain. For alloy materials such as solder, creep is also an important part, so their stress-strain curves are more complex. It has been shown that creep deformation is related to stress, strain, temperature, and time. Generally, when the temperature exceeds 35% of the melting point, creep fatigue needs to be considered [6].

ISBN 978-3-8007-6414-3

The Anand model is widely used to describe the viscoplastic behavior of solder. It describes the relationship between the strain rate and temperature and the deformation behavior of viscoplastic materials, strain hardening, the historical effect of the strain rate, and the dynamic recovery of strain [7]. Compared with other constitutive models, it uses the deformation resistance *s* as a single internal variable. The Anand model includes the inelastic flow equation and the evolution equation of internal variables, where the flow equation is:

$$\frac{d\varepsilon_p}{dt} = A\exp\left(-\frac{Q}{RT}\right)\left[\sinh\left(\zeta\frac{\sigma}{s}\right)\right]^{\frac{1}{m}} \quad (1)$$

Where $d\varepsilon_p/dt$ is inelastic strain rate, A is the pre-exponential factor, Q is the activation energy, R is the gas constant, T is the absolute temperature, ζ is the multiplier of stress, σ is the equivalent Von Mises stress, and m is the strain rate sensitivity.

The evolution equation of internal variables s is:

$$\frac{ds}{dt} = h_0\left|1-\frac{s}{s^*}\right|^a \operatorname{sign}\left(1-\frac{s}{s^*}\right)\frac{d\varepsilon_p}{dt} \quad (2)$$

Where h_0 is the hardening constant, a is the strain rate sensitivity of hardening, s^* is saturation value of deformation resistance and which can be described as:

$$s^* = s_a\left[\frac{1}{A}\frac{d\varepsilon_p}{dt}\exp\left(\frac{Q}{RT}\right)\right]^n \quad (3)$$

Where s_a is the saturation coefficient and n is the sensitivity of deformation resistance. There are a total of 9 parameters to define the Anand model.

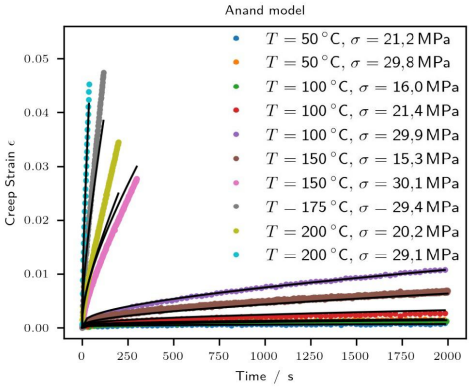

Fig. 1. Fitting effect of Anand model for sintered silver

For sintered silver, the constitutive models used in different literature are also different. One is the elastic-plastic model, considering that sintered silver belongs to metals [8], and the other is the viscoplastic model, similar to solder [9]. The latest research shows that the stress-strain relationship of the sintered layer is related to the composition ratio, porosity, temperature, etc. In [9], different constitutive models are used to fit the stress-strain curve, and found that the Anand model had the best fitting effect, as shown in Fig. 1. Therefore, the Anand model is also chosen as the constitutive model for sintered silver in this paper.

2.2 Energy-based Darveaux model

At present, there are many lifetime prediction models used in fatigue analysis, which can be roughly divided into three kinds based on different failure mechanisms: stress-based, strain-based, and energy-based models [10]. The latter is more suitable for viscoplastic materials, the viscoplastic energy dissipation can be obtained from the stress-strain hysteresis curve. The Darveaux model is the mostly used energy-based model, which divides the crack propagation into two parts: crack initiation and crack propagation, as shown in Eq.(4)~Eq.(6).

$$N_0 = K_1(\Delta W)^{K_2} \quad (4)$$

$$\frac{dl}{dN} = K_3(\Delta W)^{K_4} \quad (5)$$

$$N_f = N_0 + \frac{l_0}{K_3(\Delta W)^{K_4}} \quad (6)$$

Where N_0 is the number cycles of crack initiation, dl/dN is the crack propagation, ΔW is the average dissipated energy density during a complete temperature cycle and l_0 is the characteristic crack length corresponding to the failure criterion.

3 Fatigue model of sintered silver

Usually, the parameters of the fatigue model can be directly measured and fitted through fatigue testing, which requires separate sample preparation of the material itself. However, the material properties of nano-silver are strongly related to the sintering process, and it is difficult to ensure consistency in the porosity of sintered silver in both the prepared and actual samples, which will inevitably affect the final parameters of fatigue model. Therefore, a fatigue model parameter inversion method that combines experimental and simulation methods for actual samples is proposed in this paper. Due to the fact that the fatigue model parameters are only related to the material itself and are independent of the structure and external stress, considering the high cycle fatigue lifetime of the sintered layer, ordinary temperature cycling tests may require a longer test duration. Therefore, the liquid-to-liquid thermal shock (TS) is chosen to conduct accelerated aging tests on the sintered layer.

3.1 Liquid-to-liquid thermal shock test

Thanks to the better convective exchange provided by liquid media, liquid-to-liquid TS test which can ensure a higher temperature rate and strain rate to the device

 DOI:10.30420/566414074

under test is a reasonable methodology to exploit fatigue behavior much faster than other reliability test such as air-to-air TS or PC test. More importantly, failure analysis shows that the failure modes after the PC test and the TS test are the same, both are degradation of the topside sintered layer, as shown in Fig. 2.

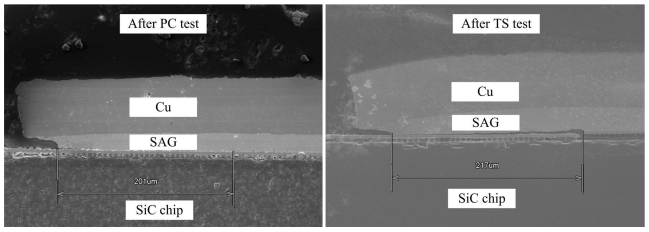

Fig. 2. Cross section of the sintered silver (SAG) after PC and TS test

The test sample is as shown in Fig. 3. There are 20 SiC chips on one substrate, which is equivalent to 20 samples in statistics. In order to further improve the experimental efficiency, 2 different thicknesses of chips (0.18mm & 0.38mm) were selected, so that 4 different thermal stress conditions can be generated under 2 experimental conditions (-40℃~150℃ & -65℃~150℃). To dynamically characterize the degree of degradation of the sintered layer, degraded area was chosen rather than crack length, which can be easily obtained from SAM images. Cross section is obviously not suitable as it would damage the sample and the crack measurements are highly dependent on the position of the cross section. To this end, samples were taken out and scanned every 500 cycles, and the results are shown in Fig. 4. Finally, a total of 3,000 cycles were performed at -40℃~150℃, and a total of 2,500 cycles were performed at -65℃~150℃.

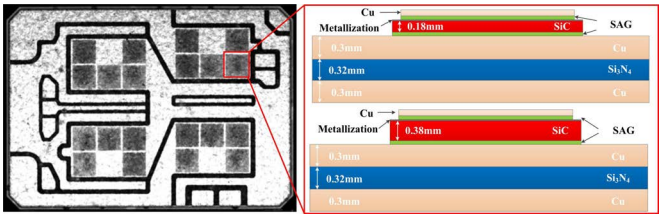

Fig. 3. Test sample in liquid-to-liquid TS test

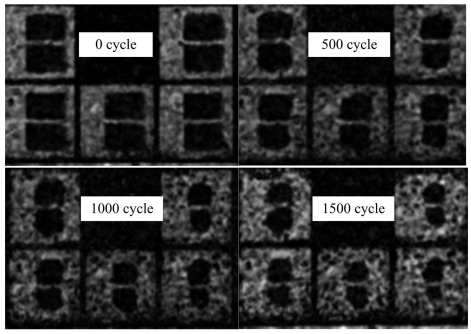

Fig. 4. SAM images after different TS cycles

The Weibull statistical results of the degraded area of all samples under different TS cycles and different test conditions are shown in Fig. 5. The scale parameter is the characteristic value of the degraded area required for modeling. Furthermore, the characteristic values of the degradation area under different cycles are plotted on a graph, as shown in Fig. 6. Assuming that the degradation is linear, the slope is the crack propagation rate dα/dN, and the intersection with the horizontal axis is the number cycles of crack crack initiation N_0. For the unrealistic situation of N_0 is less than 0, the reason is that the degradation in the early stage is relative faster and does not follow the linear degradation assumption. Ref. [11] points out that the number cycles of crack initiation can be negligible compared to that of crack propagation. In addition,it is very difficult to accurately quantify the number cycles of crack initiation in experiments. Therefore, only the process of crack propagation is considered in this paper, the final formulation of the fatigue model is:

$$\frac{d\alpha}{dN} = K_1(\Delta W)^{K_2} \tag{7}$$

$$N_f = \frac{\alpha_0}{K_1(\Delta W)^{K_2}} \tag{8}$$

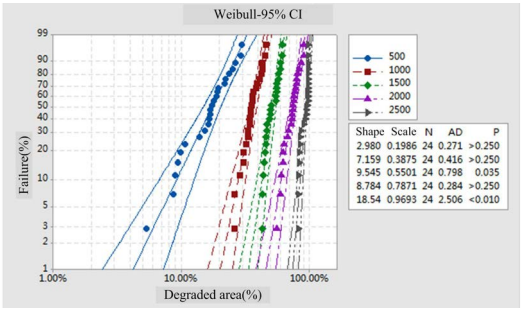

(a) 0.38mm chip (-40℃~150℃)

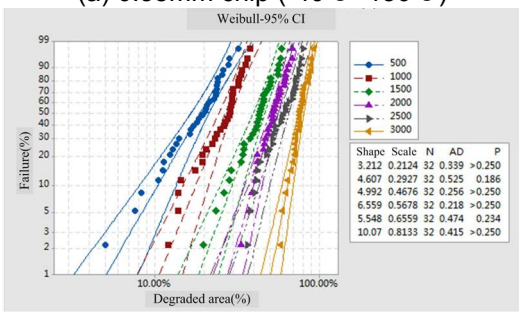

(b) 0.18mm chip (-40℃~150℃)

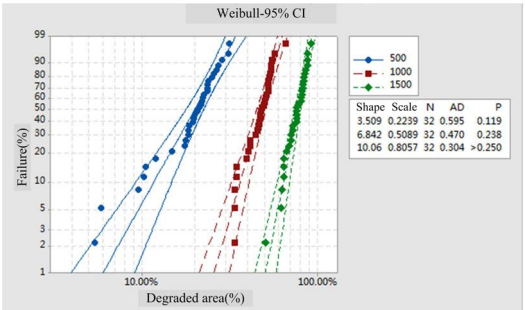

(c) 0.38mm chip (-65℃~150℃)

 DOI:10.30420/566414074

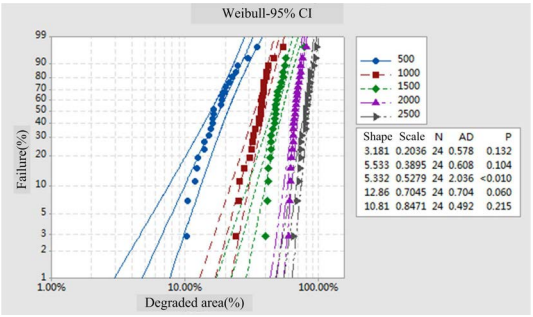

(d) 0.18mm chip (-65℃~150℃)

Fig. 5. Weibull statistical results of all samples

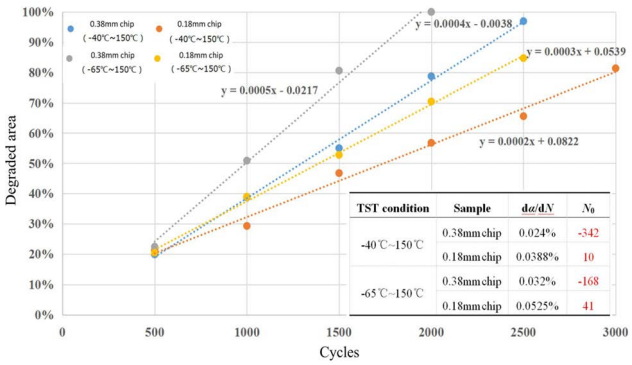

Fig. 6. Characteristic degradation area under different cycles

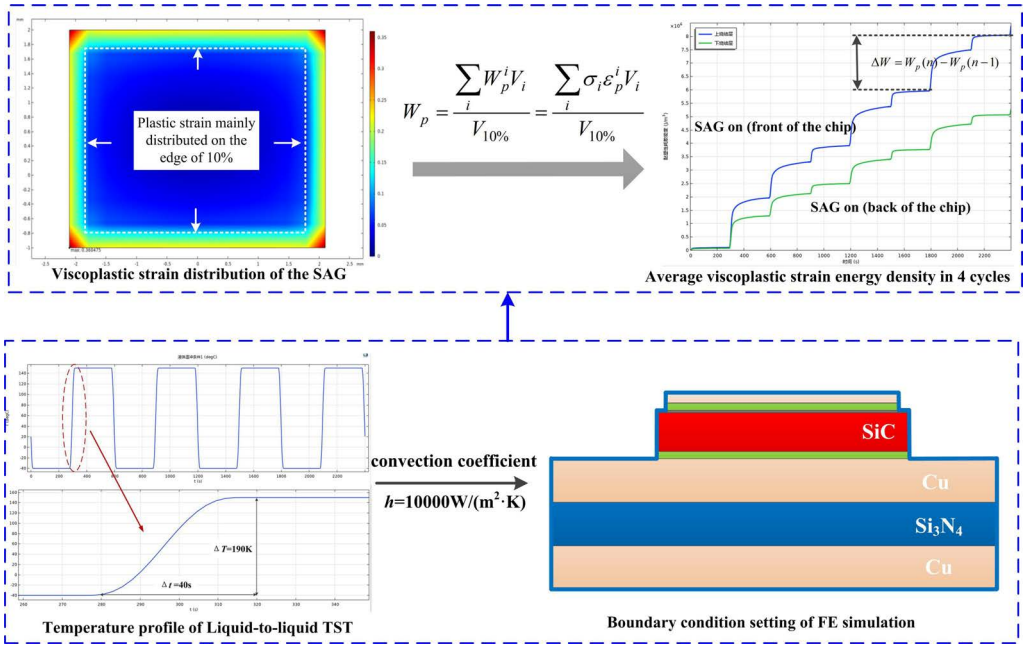

Fig. 7. Simulation model of the liquid-to-liquid TS test

3.2 Parameter inversion for fatigue model

The variable of the fatigue model is Δ*W*, which needs to be obtained through simulation. Since the substrate is isothermal during TS test, only a single-chip simulation model was established, as shown in Fig. 7. The viscoplastic deformation is mainly concentrated around the edge of the sintered layer, which is consistent with the test results. Therefore, the average dissipated energy density is calculated for the 10% area of the edge. A total of 4 cycles were simulated, and the Δ*W* of the last cycle was calculated as the model variable. Combining the test results and simulation results, taking the logarithms on both sides of the model, and performing linear fitting, the two parameters K_1 and K_2 of the fatigue model can be obtained, as shown in Fig. 8. α_0 is the characteristic degraded area corresponding to the failure criterion, which is 50% in this paper.

TST condition	Sample	Δ*W* (MJ/m³) (simulation)	d*α*/d*N* (experiment)
-40 ℃~150 ℃	0.18mm chip	1.479	0.024%
	0.38mm chip	2.071	0.0388%
-65 ℃~150 ℃	0.18mm chip	1.595	0.032%
	0.38mm chip	2.204	0.0525%

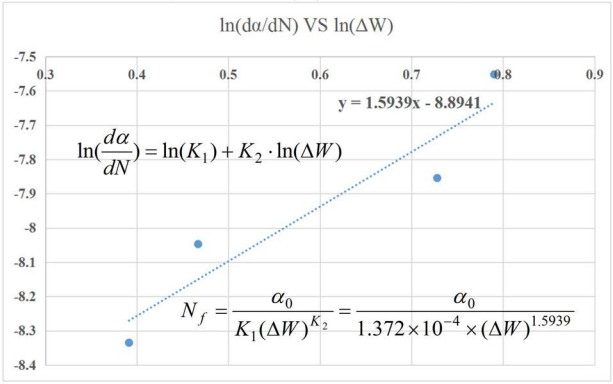

Fig. 8. Parameter inversion for fatigue model

4 Lifetime modeling subjected to PC simulations

Different from the isothermal substrate during TS test, there is a significant temperature gradient inside the module during PC test. Therefore, the simulation model needs to be established based on the entire module. The process of establishing a lifetime model is the same as in experiments, except that it is all done by simulation. Assuming that the power cycling lifetime and junction temperature swing and mean junction temperature satisfy the following functional relationship:

$$N_f = K_1 \cdot \Delta T_j^{\beta_1} \cdot e^{\frac{\beta_2}{T_{jm}+273}} \tag{9}$$

4.1 Power cycling simulation matrix

By changing the load current during power cycling simulation, different junction temperature swings can be generated. If the water temperature is kept constant, that is, the minimum junction temperature is almost constant, the mean junction temperature will also change synchronously, which does not comply with the principle of a single control variable. Therefore, the water temperature needs to be synchronously changed with the load current. Finally, the simulation results of the junction temperature change curve during the power cycling under different load currents and water temperatures are shown in Fig. 9. Similar to the liquid-to-liquid TS simulation, the ΔW of the last cycle is extracted, and substituted into the fatigue model to predict the lifetime under different PC conditions.

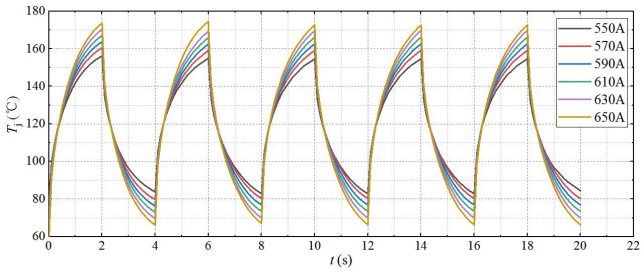

No.	I_L/A	T_w/℃	T_{jmax}/℃	T_{jmin}/℃	ΔT_j/℃	T_{jm}/℃	ΔW (MJ/m³)	N_f
1	550	76	154.5	84.5	70	119.5	0.01661	2502177
2	570	73	159	80.4	78.6	119.7	0.02080	1747724
3	590	69	162.5	77	85.5	119.75	0.02607	1219389
4	610	65	166	73.5	92.5	119.75	0.03292	840616
5	630	61	169.5	70	99.5	119.75	0.04205	569190
6	650	57	172.5	66.5	106	119.5	0.05017	429534

Fig. 9. Bias simulation results of the junction temperature swing

By controlling the load current to remain constant, the junction temperature swing can be maintained. Then, the mean junction temperature can be changed as water temperature changes. The bias simulation results of mean junction temperature are shown in Fig. 10.

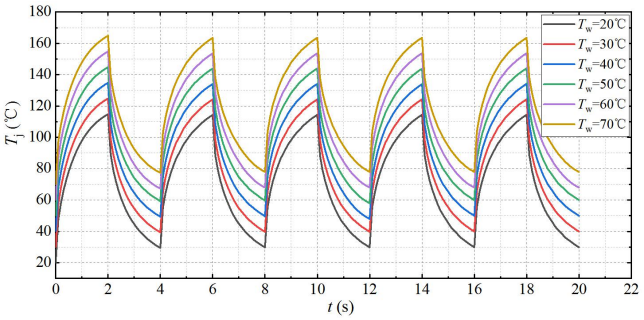

No.	I_L/A	T_w/℃	T_{jmax}/℃	T_{jmin}/℃	ΔT_j/℃	T_{jm}/℃	ΔW (MJ/m³)	N_f
1	590	20	114	30	84	72	0.01550	2792762
2		30	124	40	84	82	0.01716	2374555
3		40	134	50	84	92	0.01916	1991441
4		50	144	60	84	102	0.02144	1665867
5		60	153.5	68	85.5	110.8	0.02144	1456742
6		70	163.5	78	85.5	120.8	0.02332	1194923

Fig. 10. Bias simulation results of the mean junction temperature

4.2 Power cycling lifetime modeling

The coefficient of junction temperature swing β_1 can be fitted based on the results in Fig. 9. Since the mean junction temperature is the same, Eq. (9) can be simplified as:

$$N_f = K \cdot \Delta T_j^{\beta_1} \tag{10}$$

Take the logarithm of both sides simultaneously:

$$\ln(N_f) = \ln(K) + \beta_1 \ln(\Delta T_j) \tag{11}$$

Based on equation (11), linear fitting was performed on the data in Fig. 9, as shown in Fig. 11, β_1=-3.937.

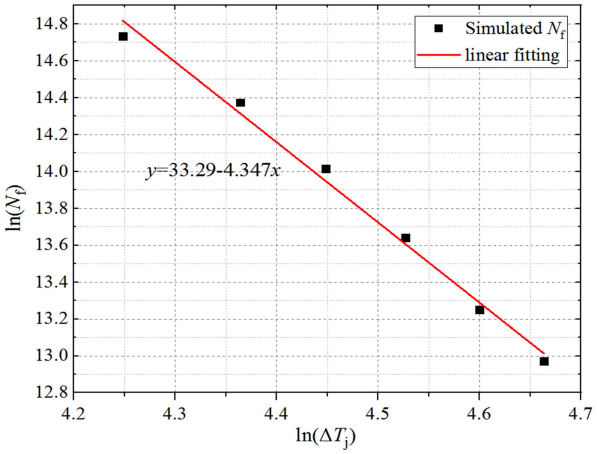

Fig. 11. Linear fitting of β_1

Then, the coefficient of mean junction temperature β_2 can be fitted based on the results in Fig. 10. Since the junction temperature swing is the same, Eq. (9) can be simplified as:

$$N_f = K \cdot e^{\frac{\beta_2}{T_{jm}+273}} \tag{12}$$

Take the logarithm of both sides simultaneously:

$$\ln(N_f) = \ln(K) + \frac{\beta_2}{T_{jm} + 273} \quad (13)$$

Based on Eq. (13), linear fitting was performed on the data, as shown in Fig. 12, β_2=2349.

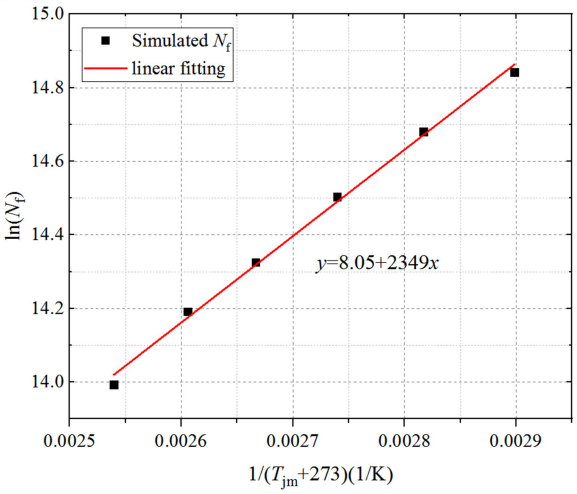

Fig. 12. Linear fitting of β_2

In summary, the power cycling lifetime model obtained from simulation matrix and fatigue model is:

$$N_f \sim \Delta T_j^{-3.937} \cdot e^{\frac{2349}{T_{jm}+273}} \quad (14)$$

5 Conclusion

To solve the problem of power cycling lifetime model of SiC MOSFET module, a physics-of-failure approach was presented in this paper. The core of this approach is the electric-thermal-mechanical finite element model and fatigue model. For the determination of fatigue model parameters, an inversion method combine with thermal shock experiment and simulation. considering the high cycle fatigue lifetime of the sintered layer, the liquid-to-liquid thermal shock is suggested to conduct accelerated aging tests. Compared to traditional lifetime modeling method based on power cycling test, physics-of-failure approach can significantly reduce the number of experiments and save costs, which is very suitable for fast lifetime prediction and reliability forward design in early design stages.

6 References

[1] K. Sheng: Maximum Junction Temperatures of SiC Power Devices, IEEE Transactions on Electron Devices, 2009, 56(2):337-342.

[2] C. Herold, M. Schaefer, F. Sauerland, T. Poller, J. Lutz, O. Schilling: Power cycling capability of Modules with SiC-Diodes, Proc. International Conference on Integrated Power Systems, 2014.

[3] A. Schiffmacher, A. Bashiti, D. Strahringer: New Lifetime Model for Advanced Power Semiconductor Interconnects, Proc. IEEE 72nd Electronic Components and Technology conference, 2022.

[4] H. Wang, M. Liserre, F. Blaabjerg: Transitioning to physics-of-failure as a reliability driver in power electronics, IEEE Journal of Emerging & Selected Topics in Power Electronics, 2014, 2(1): 97-114.

[5] JEDEC. JEP148 Reliability Qualification of Semiconductor Devices Based on Physics of Failure Risk and Opportunity Assessment, 2014.

[6] P. Vianco: Lead-free solder interconnection reliability, Detroit: ASM International, 2005.

[7] L. Anand: Constitutive equations for the rate-dependent deformation of metals at elevated temperatures, Transactions of the Asme Journal of Engineering Materials & Technology, 104(1): 12-17,1982.

[8] P. Rajaguru, K. Lu, C. Bailey: Sintered silver finite element modelling and reliability based design optimisation in power electronic module, Microelectronics Reliability, 2015, 55(6):919-930.

[9] F. Forndran, J. Heilmann, M. Metzler: Determination of Rate- and Temperature Dependent Inelastic Material Data for Sintered Silver Die Attach and Simulative Implementation, Proc. EuroSimE 2022,1-6.

[10] Y. Borui, L. Jun, W. Bo: Numerical and Experimental Investigations of the Thermal Fatigue Lifetime of CBGA Packages, Computer modeling in Engineering & Sciences, 2022, 130(2): 1113-1134.

[11] A. Sitta, G. Mauromicale, G. Sequenzia: Thermo-mechanical finite element simulation and visco-plastic solder fatigue for low voltage discrete package, Proc. EuroSimE 2021.